Essential Dynamics of DNA-Antibody Complexes

Natalia I. Akberova, Artem A. Zhmurov, Tatiana A. Nevzorova & Rustem I. Litvinov

BioNanoScience

ISSN 2191-1630
Volume 6
Number 4

BioNanoSci. (2016) 6:543-549
DOI 10.1007/s12668-016-0284-z

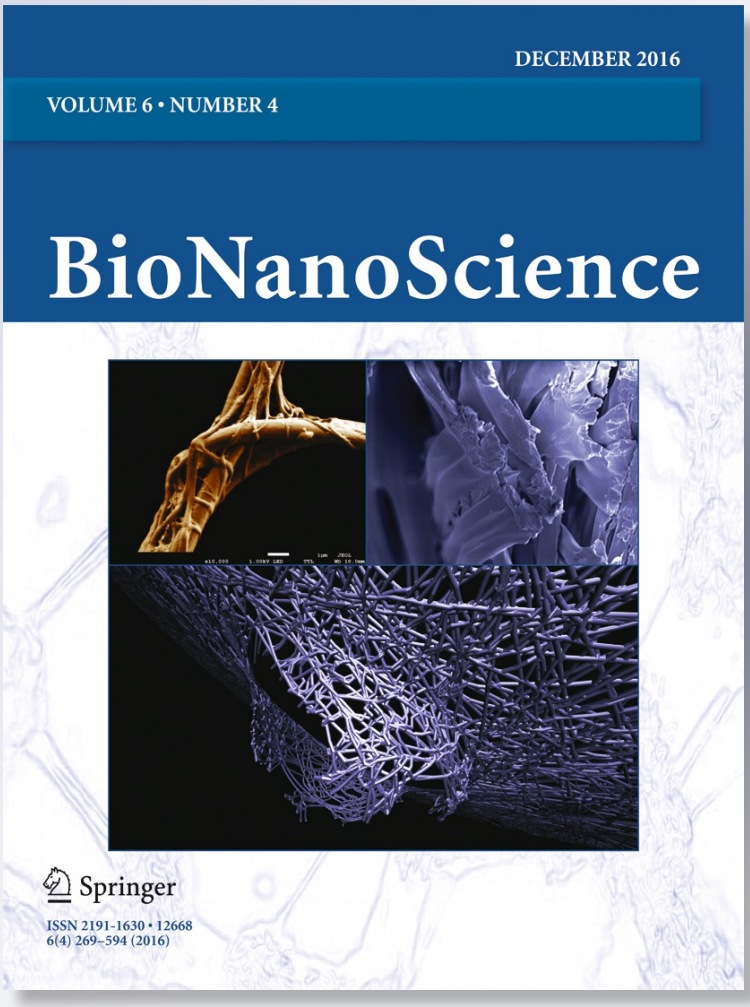

Springer

BioNanoSci. (2016) 6:543–549
DOI 10.1007/s12668-016-0284-z

Essential Dynamics of DNA-Antibody Complexes

Natalia I. Akberova[1] · **Artem A. Zhmurov**[2] · **Tatiana A. Nevzorova**[1] · **Rustem I. Litvinov**[1,3]

Published online: 21 September 2016

Abstract Antibodies against double-stranded DNA play an important role in the pathogenesis of autoimmune diseases. Structural analysis of antibody-DNA complexes contributes to our understanding of the role of DNA-containing immune complexes in human pathologies and may help in designing novel treatments. In this paper, we study dynamics of the full-atomic structure of the molecular complexes formed by an antibody *Fab* fragment with double-stranded DNA, containing or not containing a thymine dimer. Molecular dynamics simulations are used in conjunction with the Principle Component Analysis technique. We found that removing a covalent bond from the thymine dimer results in changes of the structural dynamics of the light and heavy chains of *Fab* as well as in the DNA strands. A significant increase in mobility of the *Fab* light chain was observed throughout the entire simulation runs with a higher amplitude of fluctuations at the interface with DNA. Essential dynamics analysis of simulation trajectories of the antibody-dsDNA complexes shows that fluctuations in the low-frequency eigenvectors are localized at the ends of the DNA sequences, suggesting that these bending motions are important for the DNA-antibody interactions.

✉ Rustem I. Litvinov
litvinov@mail.med.upenn.edu

[1] Kazan Federal University, 18 Kremlyovskaya St, Kazan 420008, Russian Federation

[2] Moscow Institute of Physics & Technology, 9 Institutskiy Per., Dolgoprudny, Moscow Region 141700, Russian Federation

[3] University of Pennsylvania Perelman School of Medicine, 421 Curie Blvd, Philadelphia, PA 19104-6058, USA

Keywords Anti-DNA antibody · dsDNA · Immune complex · Thymine dimer · Molecular dynamics simulation · Principal component analysis

1 Introduction

Antibodies against double-stranded DNA (dsDNA) play an important role in the pathogenesis of autoimmune diseases; for instance, anti-DNA antibodies are serological hallmarks and key molecular markers for diagnosis and estimation of disease activity in systemic lupus erythematosus [1]. Elucidation of the structural mechanisms of an antigen recognition and interaction of anti-DNA antibodies provides a basis for understanding the role of DNA-containing immune complexes in human pathologies and for developing new treatments. The crystal structure of dsDNA containing a (4–6) photoproduct in a complex with the *Fab* fragment of a monoclonal antibody 64M-5 was determined at 2.5-Å resolution [2]. However, X-ray crystallography data only show a static antibody-DNA structure, whereas the binding mechanisms in antibody–antigen interactions are dynamic in nature. Computer-based molecular dynamics (MD) simulation allows one to study the dynamic picture of antibody–antigen interactions, and interpretation of the MD trajectories can lead to better understanding of how antibodies perform their biological functions.

A MD trajectory provides snapshots depicting a protein or nucleic acid in multiple configurations with coordinates of every atom saved at a given time intervals. These conformational ensembles are best represented by a vector space that spans a large number of dimensions equal to the number of degrees of freedom. Principal component analysis (PCA) is a multivariate statistical technique applied to systematically reduce the number of dimensions needed to describe a

biopolymer dynamics through a decomposition process that filters observed motions from the largest to smallest spatial scales [3]. The process of applying PCA to a protein or nucleic acid trajectory is called essential dynamics (ED) since the "essential" motions are extracted from the set of sampled conformations. The large-scale motions are often the most biologically relevant; therefore, only a small number of PCA modes having the greatest variances are used to characterize large-scale molecular motions [4]. Experience suggests that 3–5 dimensions are often sufficient to capture over 70 % of the total variance in a given family of structures. Thus, a handful of principal components are sufficient to provide a useful description, while still retaining most of the variance in the original distribution [5].

The objective of this work was to elucidate atomic structural variations of the antibody-dsDNA complexes and the details of interaction between the antibody *Fab* fragment and the DNA strands, containing or not containing the thymine dimer, using MD simulations followed by PCA of MD trajectories. This technique previously proved to be useful in describing essential motions in the antibody [6]. Here, we apply it to extract the major components of the DNA motion.

2 Material and Methods

2.1 Preparation of Structures for MD Simulations

Three-dimensional crystal structure of a 64-M-5 *Fab*-antibody [7] bound to a dsDNA fragment containing a covalent thymine dimer was obtained from Protein Data Bank (PDB code: 3VW3) and used as a basic initial model. Amino acid residues that are not resolved in the X-ray crystallography and hence are missing in the crystal structure were added to the *Fab* fragment as previously described [6]. The light and heavy chains of the *Fab* fragment were then truncated in order to reduce the system size, with 112 and 122 residues kept in the light and heavy chains, respectively. The binding interface of the *Fab* fragment with the DNA was far from the truncated portions and remained unchanged. Two systems were prepared for MD simulations: (i) Fab-DNAtt in which a covalent bond between T9 and T10 in the DNA A-strand was retained from the original 3VW3 structure and (ii) Fab-DNA without the thymine dimer in the DNA A-strand. Both constructs were solvated in TIP3P water boxes with the dimensions of 82.5 × 70 × 140.5 Å and 75 × 72 × 120 Å, respectively. Na^+ and Cl^- ions were added at a concentration of 150 mM in order to keep a physiological ionic strength. The final dissolved Fab-DNAtt construct contained 82,648 atoms and Fab-DNA contained 65,650 atoms. We minimized the energy of the system for 100,000 steps using a combination of conjugate gradient and line search algorithms, which is a default option in NAMD [8]. Then, both constructs were heated up to 300 K with the subsequent energy equilibration.

2.2 MD Simulations

Computation and trajectory analysis were made in the NAMD 2.10 CUDA multicore program [8] with the use of the CHARMM 36 force field parameters [9, 10]. For the production run, we used a time step of 1 fs with no rigid bonds enabled. Throughout the simulation runs, the periodic boundary conditions were used. Long-range electrostatics was computed using a PME method. To control the pressure, a Berendsen barostat was enabled with a target pressure set to 1 atm. Temperature coupling was enabled and set to a target temperature of 300 K. The durations of simulation runs were >50 ns for each construct with and without the thymine dimer. Data processing and statistical analysis were performed using the R language in the RStudio software environment. We analyzed the root mean square deviations (RMSD) and root mean square fluctuations (RMSF) and made a comparison between the antibody-dsDNA constructs, containing or not containing the thymine dimer, in order to examine their structures and dynamic behavior. The DNA-*Fab* interaction energies and forces were evaluated using NAMD Energy Plugin, v. 1.4 in VMD. To study the protein and the DNA collective motions, PCA was performed on trajectories of the FabDNAtt and FabDNA constructs using the Bio3D package [5] and additional custom scripts in R and VMD [8].

3 Results and Discussion

3.1 RMSD and RMSF Analyses

The MD simulations enabled us to reveal some essential dynamic structural features of the complex formed by the antibody *Fab* fragment and the dsDNA with and without a photoproduct, the thymine dimer. In order to study convergence of both systems from the starting structure, RMSD for the *Fab* chains and DNA strands were analyzed. In the RMSD plot based on a representative trajectory, the light chain of the FabDNA construct shows an increase in RMSD values in comparison to the FabDNAtt construct observed till the end of the simulation, and its RMSD distribution clearly shifted to the right towards higher values (Fig. 1a). This increase in the mobility indicates weakening of the contacts between the *Fab* light chain and DNA when a covalent bond in the thymine dimer is deleted. As for the heavy chain (Fig. 1b), during up to a half of the simulation time, the deviation shows almost the same profile of RMSD for both constructs, after which the RMSD of the heavy chain in the FabDNAtt construct (containing the thymine dimer) rises slightly, which is reflected in the histogram (Fig. 1b). In Fig. 1c, the DNA A-strand in both constructs shows similar RMSD profiles from the start till the

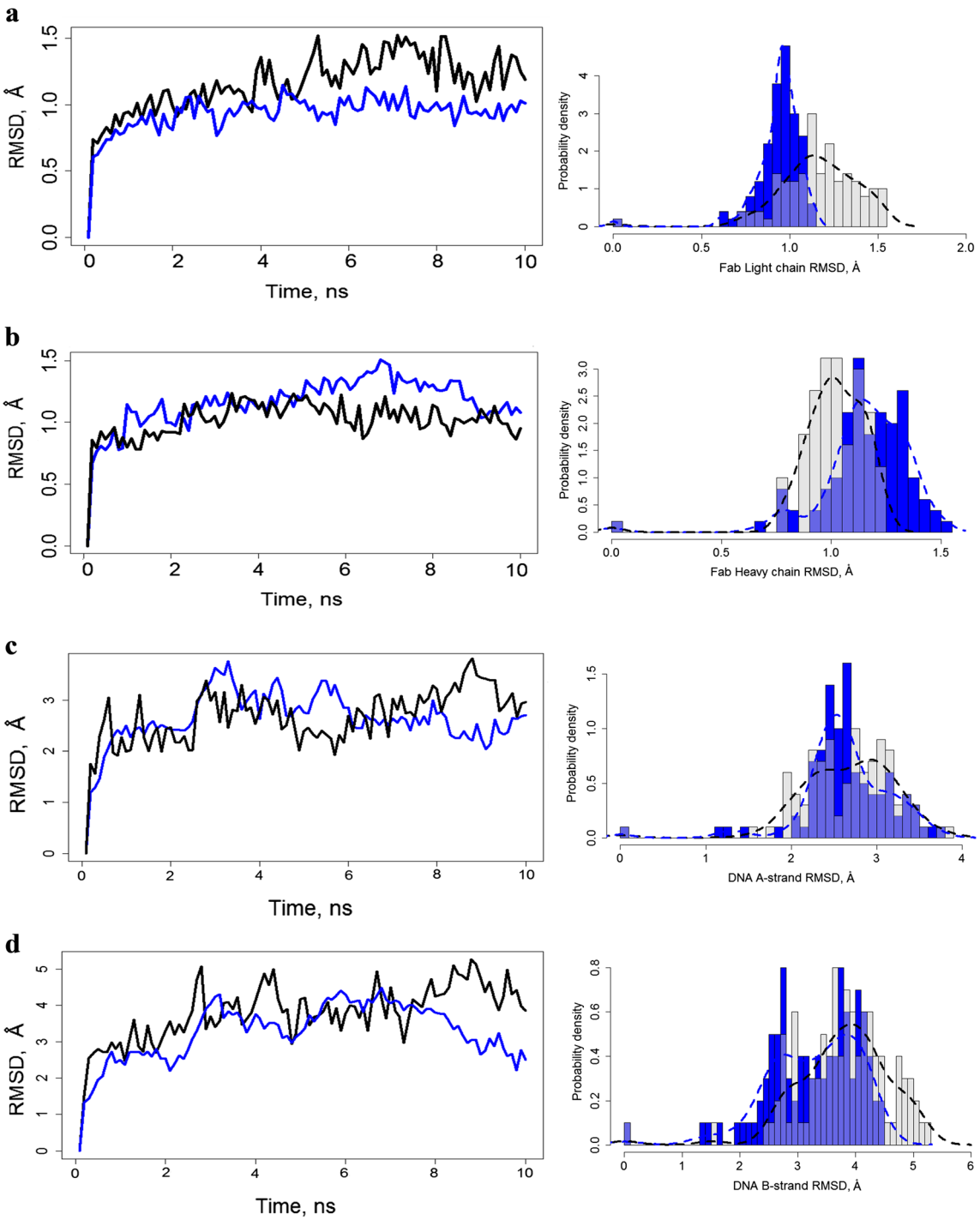

Fig. 1 *Left plots* show root mean square deviations (RMSD) as a function of time for a representative 10-ns trajectory. RMSD computed for the C_α atoms of the light (**a**) and the heavy (**b**) chains of the *Fab* fragment and for all atoms of the DNA A-strand (**c**) and B-strand (**d**). The *plots on the right* show distributions of RMSD values with the *dashed lines* representing kernel density functions. Data for the systems containing the thymine dimer (FabDNAtt) is shown in *blue*; data for systems where the thymine-thymine covalent bond was removed (FabDNA) is depicted in *black*

end of simulation, and the DNA A-chain RMSD distributions are almost the same. The A-chain in the FabDNAtt construct contains thymine dimers, which makes it rigid and bent, and the DNA strands are flipped out when the *Fab* loop is inserted [2]. Breaking a covalent bond in the thymine dimer in the FabDNA construct does not increase its flexibility, because the loop remains at the nip between the DNA strands. Compared to the A-strand, the B-strand deviations (Fig. 1d)

vary from 2.5 to 5.5 Å (versus 2 to 4 Å for the A-strand), and the B-strand in the FabDNAtt construct shows smaller deviations than in FabDNA at the end of the simulation.

To reveal the most mobile groups of atoms and to identify areas in *Fab* and DNA that undergo structural rearrangements in response to formation or breakage of the thymine dimer, we calculated the root mean square fluctuation (RMSF). RMSF analysis of the *Fab* light and heavy chains showed a lower degree of fluctuation in the area of contacts with DNA and in the LCDR3 loop for the FabDNAtt construct (Fig. 2a) compared to the FabDNA construct (Fig. 2b). This finding corroborates that the thymine dimer in DNA reduces conformational flexibility of the *Fab*-dsDNA complex and makes it more rigid, whereas removal of the covalent bond in the dimer enhances conformational flexibility of the complex.

3.2 Principal Component Analysis

We performed an essential dynamics (ED) analysis to characterize the dynamic mechanical properties of the constructs investigated. In ED analysis, we applied a simple linear transformation in the Cartesian coordinate space and the diagonalization of the covariance matrix. It yields a set of eigenvectors, which gives a vector depiction of every single component of the motion indicative of the direction of motion. Within the top eigenvectors, the first three account for a significant amount of the overall motion in each case. Each eigenvector has a corresponding eigenvalue, which describes the energetic involvement of each component into the motion. We have calculated the projection of MD trajectories for both constructs onto the first three principal components (PC1, PC2, and PC3) in phase space. The contribution of each residue of the *Fab* light and heavy chains to the first principal component shows a different phase space behavior in the constructs with and without the thymine dimer. For the *Fab* heavy chain, flexibility of the amino acids residues in the regions of contacts with DNA was reduced in FabDNAtt compared to the FabDNA construct. The phase space behavior for the *Fab* light chain in the area of contacts with DNA is less uniform. It is noteworthy that the flexibility of amino acid residues of LCDR2 in the FabDNAtt construct is increased when compared to FabDNA. ED analysis allowed estimation of the contribution of each atom of the DNA A-strand (Fig. 2a) and B-strand (Fig. 2b) to the first principal components. The DNA strands show large fluctuations at the ends, suggesting a bending motion, while the region containing the thymine dimer was more rigid. To further investigate a degree of rigidity of these fragments and to identify rigid and flexible domains in the DNA strands, we have calculated the atomic movement similarity matrix using PCA of the structural ensembles and analyzed resulting dynamics domains in VMD. In the FabDNAtt construct, the least flexible was the region that contained the thymine dimer and distorted base pairs around it (green color on Fig. 2c, d). The dynamic domains located to the left and to the right from the rigid domain (light grey and dark grey on Fig. 2c, d) perform bending motions. Since these parts of the DNA strands are complementary to each other, it is a concerted movement: when the left and right dynamic domains straighten the A-strand, they synchronically "bend" the B-strand. It is noteworthy that the most mobile nucleotide is cytosine on the B-strand's 5′-end that increases the overall degree of the B-strand flexibility (Fig. 2d). The removal of a covalent bond of the thymine dimer results in a change of structural dynamics of DNA in the complex with the *Fab* antibody fragment (Fig. 2e, f). In particular, the dynamic domain at the 3′-end of the A-strand and the complementary domain at the 5′-end of the B-strand become inflexible (Fig. 2e, f, green), while the rest of the strands, including thymines 9 and 10, undergo a concerted collective bending motion.

3.3 Energy of the Fab-DNA Interactions

Differences in the structural dynamics of the DNA strands are reflected in energy changes of the *Fab*-DNA interactions in the constructs with and without the thymine dimer. Deleting the covalent crosslinks between thymine 9 and thymine 10 in the A-strand of DNA complexed with *Fab* causes a significant increase of the noncovalent interaction energy from -389.5 ± 30.6 kcal/mol in FabDNAtt to -255.8 ± 67.6 kcal/mol in FabDNA. The analysis showed an increase in the interaction of van der Waals (VdW) energy in the construct without thymine dimer from -113.2 ± 6.6 kcal/mol in FabDNAtt to -85.7 ± 19.4 kcal/mol in FabDNA. The calculated magnitude of the electrostatic interaction between *Fab* and the DNA was -276.2 ± 28.9 kcal/mol for FabDNAtt, containing the thymine dimer, versus -170.0 ± 50.5 kcal/mol for FabDNA without the thymine dimer. The electrostatic energy dynamics (Fig. 3a) and the VdW energy dynamics (Fig. 3c) during 50-ns MD simulations clearly demonstrate that after 23-ns simulation of the equilibrium MD the electrostatic and the VdW interaction energies increase in FabDNA compared to FabDNAtt, and the energy distributions (Fig. 3b, d) display a significant increase in the electrostatic and VdW energies for the whole MD in FabDNA versus FabDNAtt (p value <2.2e-16 in a Welch Two Sample t test). We have determined the equilibrium *Fab*-DNA interaction energies earlier [6]. In this study, the *Fab* light and heavy chains have been truncated and, although the interface of the *Fab* interaction with DNA was not affected in any way, now we have identified that the removal of a covalent bond in the thymine dimer leads to switching of the binding state, as evidenced by the bimodal distribution of both electrostatic energy (Fig. 3b) and the energy of the van der Waals interactions (Fig. 3d) in the FabDNA construct without the thymine dimer. These results confirm a higher affinity of the studied anti-DNA

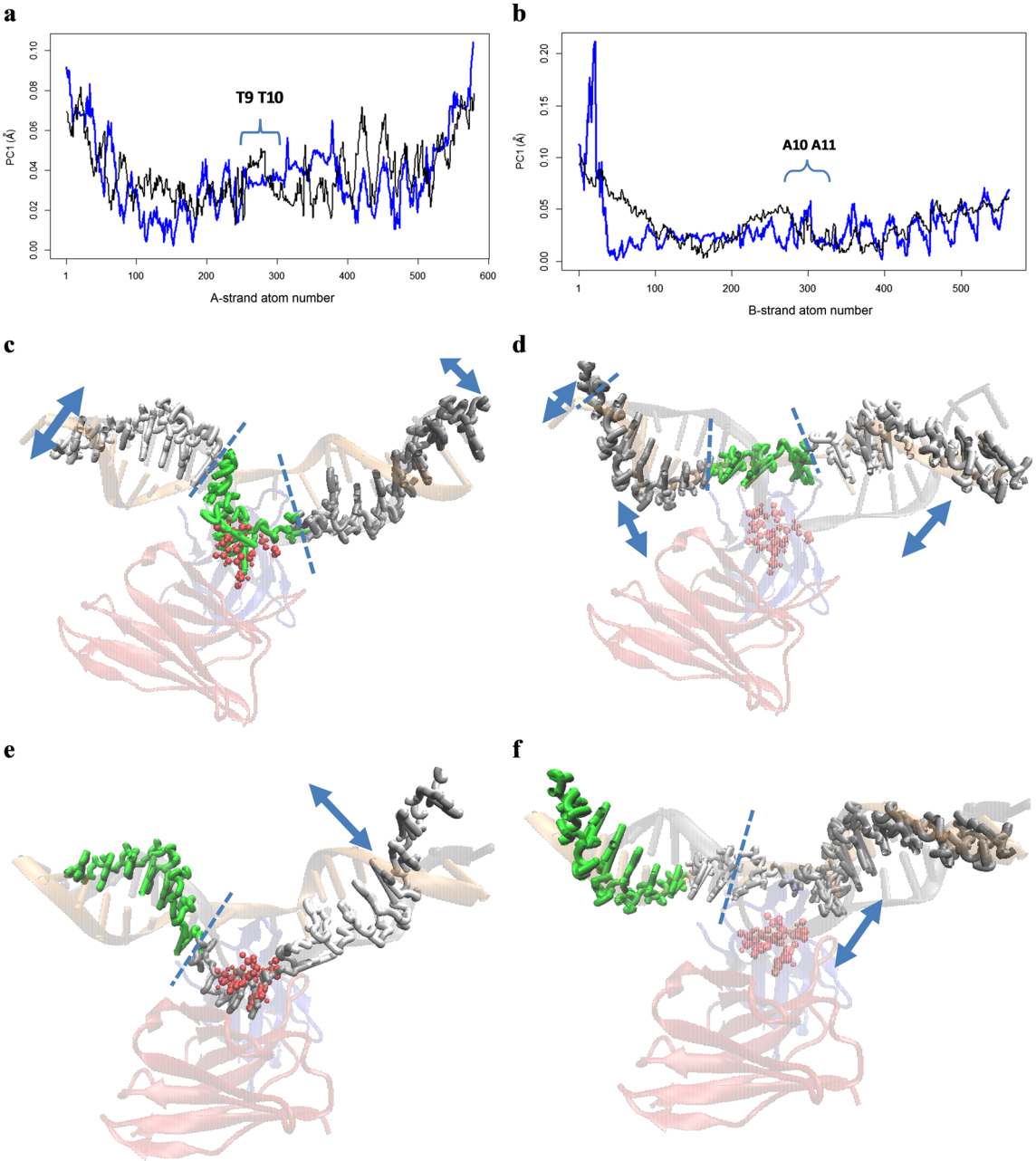

Fig. 2 Contribution of the DNA A-strand atoms (**a**) and B-strand atoms (**b**) to the first principal component for the FabDNAtt (*blue*) and the FabDNA (*black*) constructs. Location of the thymine dimer is indicated by a *brace*. **c** and **d** show domain and shear movements along the first principal component of the DNA A-strand (**c**) and B-strand (**d**) in the FabDNAtt construct. **e** and **f** show the same for the FabDNA construct. *Blue arrows* on **c** to **f** indicate the direction of essential movements; *blue lines* show the hinge regions. *Green*, *grey*, and *white colors* depict different dynamic domains; *green* shows the least flexible region. The structures of the *Fab*-DNA complexes are ghosted; thymines 9 and 10 in the A-strand are shown in a *red ball-and-stick model*

antibody to photodamaged DNA because the binding energy gets smaller when the photoadduct thymine dimer is removed. However, the remaining binding energy suggests that the interactions between the antibody and native dsDNA are still strong enough and basically correspond to the existing data about DNA-anti-DNA interactions [11–13], including DNA-hydrolyzing antibodies that have a high affinity for the substrate-antigen [14].

4 Conclusions

Using molecular dynamics simulations, we investigated at atomic-level detail the interaction between the anti-DNA antibody *Fab* fragment and double-stranded DNA. Analysis of atomic fluctuations within the *Fab*-dsDNA complexes disclosed a clear difference between the complexes that contain or not contain the thymine dimer. An increase in mobility

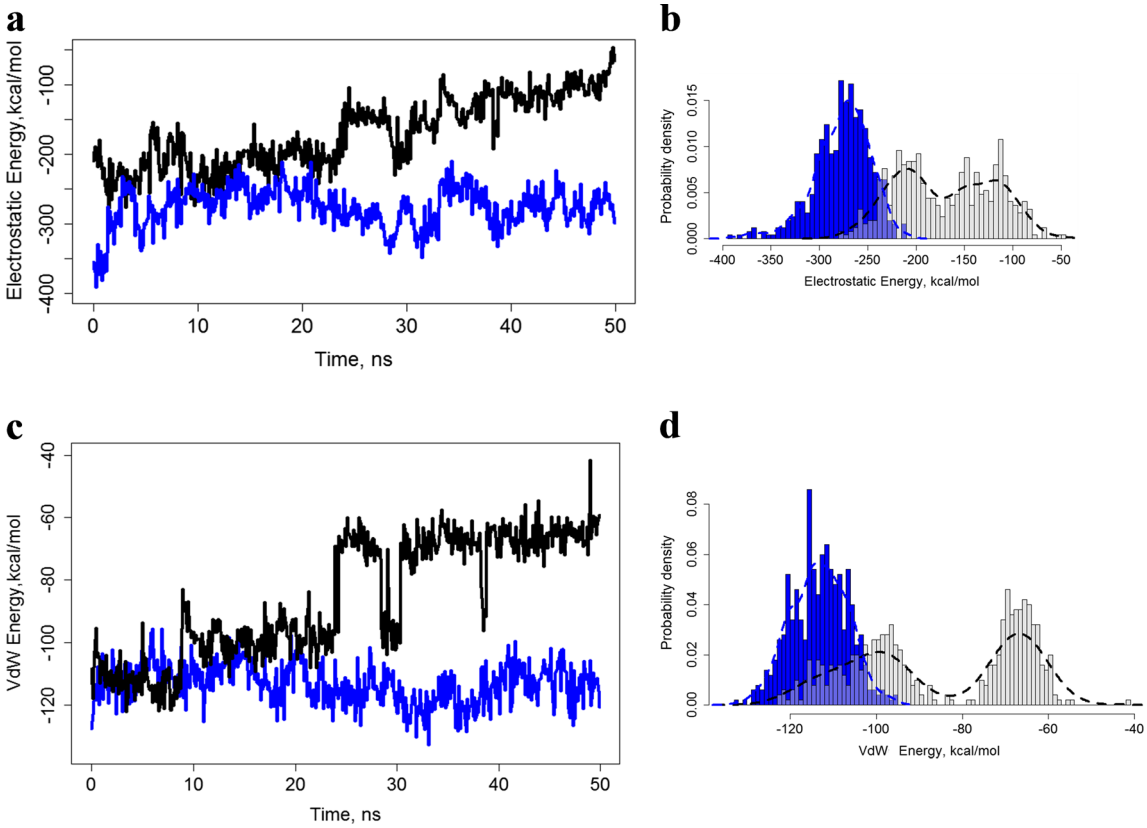

Fig. 3 The dynamics of the electrostatic energy (**a**) and its corresponding distributions with the *dashed lines* representing kernel density (**b**). The data for the *Fab* DNA interaction in FabDNAtt are shown in *blue*, for FabDNA are in *black*. **c** and **d** depict the dynamics of the Van der Waals energy (**c**) and its corresponding distributions with kernel density (**d**) The data were collected throughout a 50-ns MD simulation run

of the *Fab* light chain and the DNA strands upon deletion of the thymine dimer was shown, indicating weakening of the contacts between *Fab* and DNA when the covalent thymine-thymine bond is removed. The latter structural modification also causes a significant decrease of the binding energy, both in its electrostatic and Van der Waals components. Essential dynamics of the DNA strands in the *Fab*-dsDNA complexes shows that fluctuations are localized at the ends of the DNA strands, which corresponds to an increase in the amplitude of the bending motion.

Acknowledgments This work was supported by the Program for Competitive Growth at Kazan Federal University.

References

1. Pisetsky, D. S. (2016). Anti-DNA antibodies—quintessential biomarkers of SLE. *Nature Reviews Rheumatology, 12*(2), 102–110.
2. Yokoyama, H., Mizutani, R., Satow, Y. (2013). Structure of a double-stranded DNA (6–4) photoproduct in complex with the 64M-5 antibody Fab. *Acta Crystallogr D Biol Crystallogr, D69*, 504–512.
3. David, C. C., & Jacobs, D. J. (2014). *Methods in Molecular Biology, 1084*, 193–226.
4. Berendsen, H. J., & Hayward, S. (2000). Collective protein dynamics in relation to function. *Current Opinion in Structural Biology, 10*, 165–169.
5. Grant, B. J., Rodrigues, A., ElSawy, K., McCammon, J., Caves, L. (2006). Bio3d: an R package for the comparative analysis of protein structures. *Bioinformatics, 22*, 2695–2696.
6. Akberova, N. I., Zhmurov, A. A., Nevzorova, T. A., Litvinov, R. I. (2016). An anti-DNA antibody prefers damaged dsDNA over native. *Journal of Biomolecular Structure and Dynamics, 11*, 1–14.
7. Kobayashi, H., Morioka, H., Tobisawa, K., Torizawa, T., Kato, K., Shimada, I., et al. (1999). Probing the interaction between a high-affinity single-chain Fv and a pyrimidine (6–4) pyrimidone photodimer by site-directed mutagenesis. *Biochemistry, 38*, 532–539.
8. Phillips, J. C., Braun, R., Wang, W., Gumbart, J., Tajkhorshid, E., Villa, E., et al. (2005). Scalable molecular dynamics with NAMD. *Journal of Computational Chemistry, 26*, 1781–1802.
9. Foloppe, N., & MacKerell, A. D. (2000). All-atom empirical force field for nucleic acids: I parameter optimization based on small molecule and condensed phase macromolecular target data. *Journal of Computational Chemistry, 21*, 86–104.
10. MacKerell, A. D., Bashford, D., Bellott, M., Dunbrack, R. L., Evanseck, J. D., Field, M. J., et al. (1998). All-atom empirical potential for molecular modeling and dynamics studies of proteins. *The Journal of Physical Chemistry, 102*, 3586–3616.
11. Jang, Y. J., & Stollar, B. D. (2003). Anti-DNA antibodies: aspects of structure and pathogenicity. *Cellular and Molecular Life Sciences, 60*, 309–320.

12. Collis, A. V., Brouwer, A. P., Martin, A. C. (2003). Analysis of the antigen combining site: correlations between length and sequence composition of the hypervariable loops and the nature of the antigen. *Journal of Molecular Biology, 325*, 337–354.
13. Miyazaki, S., Shimura, J., Hirose, S., Sanokawa, R., Tsurui, H., Wakiya, M., et al. (1997). Is structural flexibility of antigen-binding loops involved in the affinity maturation of anti-DNA antibodies? *International Immunology, 9*, 771–777.
14. Gololobov, G. V., Chernova, E. A., Schourov, D. V., Smirnov, I. V., Kudelina, I. A., Gabibov, A. G. (1995). Cleavage of supercoiled plasmid DNA by autoantibody Fab fragment: application of the flow linear dichroism technique. *Proceedings of the National Academy of Sciences of the United States of America, 92*, 254–257.